Density Functional Study on the Mechanism of the Oxidative Addition of the Highly Polarized Sn−C σ-Bond to the (LH₃)(L′H₃)Pd and (LH₂C₂H₄LH₂)Pd (L, L′ = N, P, As, Sb) Complexes

Toshiaki Matsubara*

Fukui Institute for Fundamental Chemistry, Kyoto University, 34-4 Takano-Nishihiraki-cho, Sakyo-ku, Kyoto 606-8103, Japan

The electronic effect on the activation mechanism of the highly polarized Sn−C σ-bond is theoretically examined by means of a density functional method (B3LYP) using palladium model complexes with various ligands, (LH₃)(L′H₃)Pd and (LH₂C₂H₄LH₂)Pd (L, L′ = N, P, As, Sb). The author has recently reported a novel activation mechanism of the highly polarized Sn−C σ-bond of SnH₃C≡CH in a previous paper (Matsubara et al. *Organometallics* **2002**, *21*, 4482−4489). The Sn−C σ-bond approaches the Pd perpendicularly to the P−Pd−P plane of (PH₃)₂Pd, and the activation of the Sn−C σ-bond takes place by two steps via the unique intermediate **2P**, because the apical site of the palladium complex plays an important role in the activation. When the phosphine ligand is replaced by the more σ-donative nitrogen ligand or the chelate ligand, the mechanism is drastically changed, and the activation of the Sn−C σ-bond occurs in the L−Pd−L′ plane throughout by one step from the π-complex. In contrast, in the case of the substrate SnH₃(H)C=CH₂, the activation of the Sn−C σ-bond starts from the π-complex independent of the ligands. However, the reaction proceeds by the perpendicular approach of the Sn−C σ-bond with the support of the apical site, which is accompanied by the clockwise or the counterclockwise rotation of the coordinated substrate. It was found that the counterclockwise rotation, where the apical site effectively contributes to the reaction, was energetically more favorable.

1. Introduction

The activation of σ-bonds by transition metal complexes has attracted much attention from many chemists for a long time, because it very often becomes a key step of organic syntheses. Therefore, a large amount of effort has been devoted to explore the active transition metal complexes, and various types of early and late transition metal complexes are known to exhibit activation activity.[1] Oxidative addition of H−H and C−H σ-bonds of H₂ and CH₄ molecules to the phosphine-coordinated complexes (PH₃)₂M (M = Pd, Pt) is one of the most typical reactions that was found at the beginning. Many computational analyses have showed that the H−H and C−H axes of the substrates approach the metal parallel to the P−Pd−P plane formed by the bend of the P−Pd−P axis, and the breaking of these σ-bonds proceeds in the P−Pd−P plane throughout the reaction,[2,3] as illustrated below.
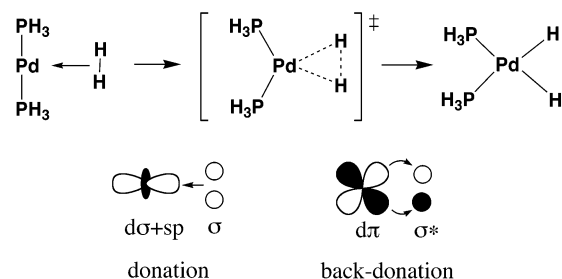
The reason is obvious when we look at the molecular orbital interactions between the metal and the σ-bond in the transition state. The electron back-donation from the occupied dπ orbital of the Pd to the σ* orbital in addition to the electron donation from the σ orbital to the unoccupied dσ+sp hybridized orbital of the Pd is required to break the σ-bond. This electron back-donation occurs from the dπ orbital in the P−Pd−P plane, because it is enhanced in energy by the electron-donative phosphine ligands. Thus, the theorists believe that the "parallel approach" of the σ-bond is a typical style of σ-bond activation on the d¹⁰ transition metal complexes (PH₃)₂M, although there exist some cases where the transition states deviate from the square-planar structure for steric reasons.[4]

* Corresponding author.
(1) For example, see: (a) Muetterties, E. L.; Rhodin, T. N.; Band, E.; Brucker, C. F.; Pretzer, W. R. *Chem. Rev.* **1979**, *79*, 91. (b) Shilov, A. E. *The Activation of Saturated Hydrocarbons by Transition Metal Complexes*; D. Reidel: Dordrecht, 1984. (c) Crabtree, R. H. *Chem. Rev.* **1985**, *85*, 245. (d) Cotton, F. A.; Wilkinson, G. In *Advanced Inorganic Chemistry*, 5th ed.; John Wiley & Sons: New York, 1988. (e) Crabtree, R. H. In *The Organometallic Chemistry of the Transition Metals*, 2nd ed.; John Wiley & Sons: New York, 1994.
(2) (a) Low, J. J.; Goddard, W. A., III. *J. Am. Chem. Soc.* **1984**, *106*, 6928. (b) Obara, S.; Kitaura, K.; Morokuma, K. *J. Am. Chem. Soc.* **1984**, *106*, 7482.

(3) (a) Low, J. J.; Goddard, W. A., III. *J. Am. Chem. Soc.* **1984**, *106*, 8321. (b) Low, J. J.; Goddard, W. A., III. *Organometallics* **1986**, *5*, 609. (c) Low, J. J.; Goddard, W. A., III. *J. Am. Chem. Soc.* **1986**, *108*, 6115.
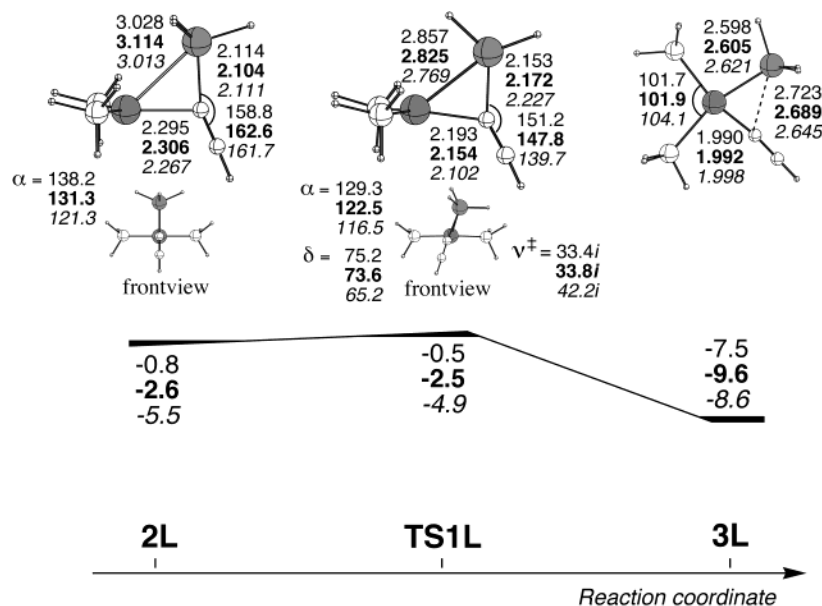
Figure 1. B3LYP/BSII potential energy surface (in kcal/mol) of the oxidative addition of the Sn–C σ-bond of $SnH_3C\equiv CH$ to the $(LH_3)_2Pd$ (L = P, As, Sb) complexes **1**, together with the optimized structures (in Å and deg) of the intermediates **2**, the transition states **TS1**, and the products **3** at the B3LYP/BSI level. The imaginary frequency (in cm^{-1}) is shown for the transition states **TS1**. α and δ represent the angle ∠L–Pd–L and the dihedral angle ∠L–m–Pd–Sn (m is the midpoint between two L atoms), respectively. The numbers in normal, bold face, and italic type are for L = P, As, and Sb, respectively.

However, the author has recently reported a unique σ-bond activation by the "perpendicular approach" of the σ-bond for the $(PH_3)_2M$ (M = Ni, Pd, Pt) + $SnH_3C\equiv CH$ system.[5] This reaction consists of two processes, as presented in Figure 1. In the first stage, the Sn–C σ-bond of the substrate $SnH_3C\equiv CH$ approaches perpendicularly to the P–Pd–P plane to form the intermediate **2P**. Here, the C atom bonded to the Sn coordinates to the Pd and is located at the equatorial position in the P–Pd–P plane, while the Sn atom has an interaction with the Pd at the apical site to keep the perpendicular form of **2P**. The Sn–C σ-bond is preliminary activated by η^2-coordination to the Pd atom. The style of coordination is thought to be completely different from the conventional η^2-C–H coordination called agostic interaction. There are two important facts worthwhile to note. One is that the Pd–C distance is very short, indicating a bonding of the C atom with the Pd atom. The other is that the C atom that coordinates to the Pd has the π orbital directed to the Pd. The Sn–C σ-bond of $SnH_3–CH_3$ without the π orbital on the C atom never forms an intermediate such as **2P** during the bond breaking.[6] In the second stage, the Sn–C σ-bond starts the rotation around the Pd–C axis, so that the Sn–C σ-bond is broken and the trigonal-pyramid-like structure is transformed to the square-planar structure. The energy barrier required for the step from **2P** to **3P** is only <1 kcal/mol despite the drastic change of the structure. This suggests a heterolytic cleavage of the highly polarized Sn–C σ-bond that is composed of two processes. The first step is the coordination of the negatively charged C atom to the Pd by electron donation with the support of the π orbital. Thereby, the polarization of the Sn–C σ-bond is further encouraged.

The second step is the migration of the positively charged Sn to the occupied dπ orbital of the Pd enhanced in energy in the P–Pd–P plane.

On the other hand, the activation of the Sn–C σ-bond of stannole $(C_4H_4)SnH_2$ passes through not the Sn–C η^2-complex but the C=C π-complex.[6,7] However, the Sn–C σ-bond approaches perpendicularly to the P–Pd–P plane before breaking, and similarly the apical site of the Pd complex effectively contributes to the Sn–C σ-bond cleavage.

In the present study, to examine in further detail this unique activation mechanism of the highly polarized Sn–C σ-bond, computations were performed for the substrates $SnH_3C\equiv CH$ and $SnH_3(H)C=CH_2$ using a density functional method (B3LYP). As the palladium complex, two models, $(LH_3)(L'H_3)Pd$ and $(LH_2C_2H_4LH_2)$-Pd, were adopted, and four atoms, N, P, As, and Sb, which belong to the same group, were used for L to systematically know the electronic effect of the ligand on the activation mechanism. We can expect some changes in the activation reaction, because the key orbitals of the Pd for the interaction with the Sn–C σ-bond are electronically influenced by the various ligands. In fact, the electronic character of the ligand was reflected in the activation of the Sn–C σ-bond, and the most electron-donative nitrogen ligand showed a peculiar mechanism. The factor determining the mechanism of the Sn–C σ-bond activation that was recently successfully applied to organic syntheses as a key step[8] is discussed in detail in the present paper.

Following an explanation of the computational procedures, the activation of the Sn–C σ-bond of $SnH_3C\equiv CH$ is first discussed in section 3.1. In section 3.2, the activation of the Sn–C σ-bond of $SnH_3(H)C=CH_2$ is discussed. Conclusions are summarized in the last section.

(4) Sakaki, S.; Mizoe, N.; Musashi, Y.; Biswas, B.; Sugimoto, M. *J. Phys. Chem. A* **1998**, *102*, 8027.

(5) Matsubara, T.; Hirao, K. *Organometallics* **2002**, *21*, 4482.

(6) Matsubara, T.; Hirao, K. *Organometallics* **2002**, *21*, 2662.

(7) Sahnoun, R.; Matsubara, T.; Yamabe, T. *Organometallics* **2000**, *19*, 5661.

Table 1. Optimized Geometric Parameters and Relative Energies (RE) of the Reactant 1P, the Intermediate 2P, the Transition State TS1P, and the Product 3P of the Path 1P → 2P → TS1P → 3P, Calculated at Different Levels

	geometric parameters[a] (Å and deg)					RE[b] (kcal/mol)
	Pd−Sn	Pd−C	Sn−C	α	δ	
1P			2.080/2.077	180.0/180.0		0.0/0.0/0.0
2P	3.028/3.280	2.295/2.468	2.114/2.096	138.2/132.9	90.0/89.5	−0.3/−0.8/−1.4
TS1P	2.857/2.847	2.193/2.155	2.153/2.185	129.3/123.1	75.2/65.4	−0.2/−0.5/−0.6
3P	2.598/2.616	1.990/2.005	2.723/2.712	101.7/105.5	0.0/0.0	−9.5/−7.5/−7.9

[a] The numbers on the left- and right-hand sides of the slash are for the B3LYP/BSI and the B3LYP/BSII levels, respectively. α and δ are the angle ∠P−Pd−P and the dihedral angle ∠P−m−Pd−Sn (m is the midpoint between two P atoms), respectively. See Figure 1 for the structures. [b] The numbers on the left-, the middle, and the right-hand sides of the slash are for the B3LYP/BSI//B3LYP/BSI, the B3LYP/BSII//B3LYP/BSI, and the B3LYP/BSII//B3LYP/BSII levels, respectively.

2. Computational Procedures

All calculations were performed using the Gaussian98 program.[9] The calculations of energetics as well as geometry optimizations were carried out at the B3LYP level of theory, which consists of a hybrid Becke + Hartree−Fock exchange and a Lee−Yang−Parr correlation functional with nonlocal corrections.[10] The basis set BSI used for the optimization is the lanl2dz level for all atoms, H, C, N, P, As, Pd, Sn, and Sb. To obtain more reliable energies, we used the higher level basis set BSII, i.e., 6-31G** for the H and C atoms of the substrates $SnH_3C≡CH$ and $SnH_3(H)C=CH_2$ and 6-31G* for the H, C, N, P, and As atoms of the spectator ligands LH_3 and $(LH_2C_2H_4-LH_2)$ (L = N, P, As). For Pd, the triple-ζ valence basis functions augmented by an additional single set of f orbitals with exponents of 1.472[11] and the effective core potential (ECP) determined by Hay−Wadt[12] to replace the core electrons except for the 18 electrons in the valence shell and, for Sn and Sb, the (3s,3p)/[2s,2p] basis functions with a polarization function, i.e., 5d with the exponents 0.183 (Sn)[13] and 0.211 (Sb),[13] and the Hay−Wadt ECP[14] to replace the 46 core electrons except for the valence electrons were used. In the previous paper, the B3LYP/BSII level was adopted for the optimization.[5] However, the shape of the potential energy surface, the structural features of the intermediate, the transition state, and the product, and the nature of the bonding are well reproduced even at the B3LYP/BSI level, as presented in Table 1 for the path 1P → 2P → TS1P → 3P. Therefore, in the present study, the optimization was performed at the B3LYP/BSI level and the energy was improved by single-point calculations at the B3LYP/BSII level.

(8) For example, see: (a) Shirakawa, E.; Yoshida, H.; Hiyama, T. *Tetrahedron Lett.* **1997**, *38*, 5177. (b) Shirakawa, E.; Yoshida, H.; Kurahashi, T.; Nakao, Y.; Hiyama, T. *J. Am. Chem. Soc.* **1998**, *120*, 2975. (c) Yoshida, H.; Shirakawa, E.; Kurahashi, T.; Nakao, Y.; Hiyama, T. *Organometallics* **2000**, *19*, 5671. (d) Shirakawa, E.; Hiyama, T. *J. Organomet. Chem.* **1999**, *576*, 169, and references therein.

(9) Frisch, M. J.; Trucks, G. W.; Schlegel, H. B.; Scuseria, G. E.; Robb, M. A.; Cheeseman, J. R.; Zakrzewski, V. G.; Montgomery, J. A., Jr.; Stratmann, R. E.; Burant, J. C.; Dapprich, S.; Millam, J. M.; Daniels, A. D.; Kudin, K. N.; Strain, M. C.; Farkas, O.; Tomasi, J.; Barone, V.; Cossi, M.; Cammi, R.; Mennucci, B.; Pomelli, C.; Adamo, C.; Clifford, S.; Ochterski, J.; Petersson, G. A.; Ayala, P. Y.; Cui, Q.; Morokuma, K.; Malick, D. K.; Rabuck, A. D.; Raghavachari, K.; Foresman, J. B.; Cioslowski, J.; Ortiz, J. V.; Stefanov, B. B.; Liu, G.; Liashenko, A.; Piskorz, P.; Komaromi, I.; Gomperts, R.; Martin, R. L.; Fox, D. J.; Keith, T.; Al-Laham, M. A.; Peng, C. Y.; Nanayakkara, A.; Gonzalez, C.; Challacombe, M.; Gill, P. M. W.; Johnson, B. G.; Chen, W.; Wong, M. W.; Andres, J. L.; Gonzalez, C.; Head-Gordon, M.; Replogle, E. S.; Pople, J. A. *Gaussian 98*; Gaussian, Inc.: Pittsburgh, PA, 1998.

(10) (a) Lee, C.; Yang, W.; Parr, R. G. *Phys. Rev. B* **1988**, *37*, 785. (b) Becke, D. *J. Chem. Phys.* **1993**, *98*, 5648.

(11) Ehlers, A. W.; Böhme, M.; Dapprich, S.; Gobbi, A.; Höllwarth, A.; Jonas, V.; Köhler, K. F.; Stegmann, R.; Veldkamp, A.; Frenking, G. *Chem. Phys. Lett.* **1993**, *208*, 111.

(12) Hay, P. J.; Wadt, W. R. *J. Chem. Phys.* **1985**, *82*, 299.

(13) Huzinaga, S. *Physical Sciences Data 16, Gaussian Basis Sets for Molecular Calculations*; Elsevier: Amsterdam, 1984.

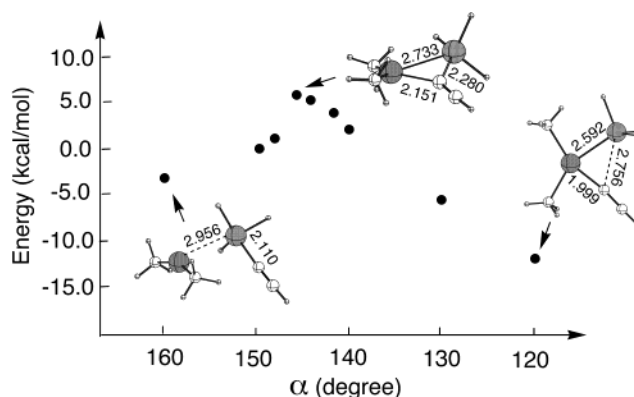(14) Wadt, W. R.; Hay, P. J. *J. Chem. Phys.* **1985**, *82*, 284.

Figure 2. Plots of the energy versus the ∠N−Pd−N angle α for the oxidative addition of the Sn−C σ-bond of $SnH_3C≡CH$ to the $(NH_3)_2Pd$ complex **1N**. The energy at each point was calculated at the B3LYP/BSI level by optimizing the structure with the frozen angle α and the Pd−N distance of 2.116 Å. The optimized structures (in Å) at the point on the top and the reactant and product sides of the energy surface are displayed together.

Table 2. Optimized Geometric Parameters and NBO Analysis of the Free $XH_3C^1≡C^2H$ and $XH_3(H)C^1=C^2H_2$ (X = Sn, C) at the B3LYP/BSI Level

	bond distance (Å)	atomic charge		X−C[1] bond %X
	X−C[1]	X	C[1]	
	$XH_3C^1≡C^2H$			
X = Sn	2.080	1.220	−0.548	24.7
C	1.472	−0.009	−0.696	50.2
	$XH_3(H)C^1=C^2H_2$			
X = Sn	2.127	1.185	−0.684	27.9
C	1.521	−0.672	−0.181	50.8

All equilibrium structures and transitions states were fully optimized without any symmetry restrictions unless otherwise indicated and identified by the number of imaginary frequencies calculated from the analytical Hessian matrix. All the reaction coordinates were followed from the transition state to the reactant and the product by the intrinsic reaction coordinate (IRC) technique.[15] On the optimization at each point presented in Figure 2 for the reaction system $(NH_3)_2Pd$ + $SnH_3C≡CH$, the Pd−N distances were arbitrary frozen to 2.116 Å (this number is the optimized distance for the free $(NH_3)_2Pd$), because one of the NH_3 ligands dissociates and goes away during the optimization. The structures were optimized at the various angles α in Tables 4 and 5. The free LH_3 (L = N, P, As, Sb) presented in Table 3 were also optimized. In all the reaction systems, the energies relative to the free (LH_3)-$(L'H_3)Pd$ and $(LH_2C_2H_4LH_2)Pd$ (L, L' = N, P, As, Sb) complexes **1** and the free substrates $SnH_3C≡CH$ and $SnH_3(H)C=CH_2$ are presented.

(15) Fukui, K.; Kato, S.; Fujimoto, H. *J. Am. Chem. Soc.* **1975**, *97*, 1.

Table 3. NBO Analysis of the Free LH₃ at the B3LYP/BSI Level

|	atomic charge		AO population		L−H bond
L	L	H	L(p_x)	H(s)	%L
N	−1.168	0.389	1.963	0.610	69.5
P	0.044	−0.015	1.478	1.014	49.3
As	0.211	−0.071	0.876	1.070	46.5
Sb	0.507	−0.169	0.774	1.169	41.5

NBO analysis[16] was performed to obtain the atomic orbital (AO) population and the charge. The binding energy (BE) of the substrate with the palladium was calculated as follows; BE = E[(ligand)Pd(substrate)] − E[(ligand)Pd]$_{distorted}$ − E[substrate]$_{distorted}$. The suffixes **N**, **P**, **NP**, **PN**, **As**, **Sb**, **cN**, and **cP** for the complexes with the ligands (NH₃)₂, (PH₃)₂, (NH₃)-(PH₃), (PH₃)(NH₃), (AsH₃)₂, (SbH₃)₂, NH₂C₂H₄NH₂, and PH₂C₂H₄PH₂ were used to label the structures.

3. Results and Discussion

The activation of the Sn−C σ-bond of the substrates SnH₃C≡CH and SnH₃(H)C=CH₂ is discussed in sections 3.1 and 3.2, respectively. Preliminary information on the Sn−C σ-bond of SnH₃C≡CH and SnH₃(H)C=CH₂ and the LH₃ ligands required for the discussion is summarized in Tables 2 and 3, respectively. As shown by the atomic charges of the Sn and the C¹ atoms (Table 2), the Sn−C σ-bonds of both SnH₃C≡CH and SnH₃-(H)C=CH₂ are highly polarized. The electron in the Sn−C bonding orbital is extremely localized on the C¹ atom. This polarization obviously originates from the nature of the Sn atom. When the Sn atom is replaced by the C atom, polarization does not occur at all. On the other hand, in Table 3 one can find a trend in the electronic character of the ligands LH₃ that depends on the atoms L. The electronegativity of L[17] is sharply reflected in the electron distribution on LH₃, and the electron density on L increases in the order N > P > As > Sb. On the basis of the value of the AO population of p_x, the strength of the electron donation from the lone pair electron of p_x to the Pd for the coordination is predicted as follows: N > P > As > Sb.

The (LH₃)(L′H₃)Pd fragments were also optimized with a variety of ∠L−Pd−L′ angles α, 180°, 150°, 120°, and 90°, although the L−Pd−L′ axis is linear in the equilibrium structure. When the L−Pd−L′ axis is linear, the bond distance of Pd−L increases with the sequence Sb > As > P > N, and the bonding energy of LH₃ decreases with the reversed sequence, N > P > As > Sb, as shown in Table 4. This is ascribed to the electron donation ability of the LH₃ ligand mentioned above. However, it is interesting that the bonding energy of NH₃ is significantly reduced when the angle α becomes less than 180°. As a result, the bonding energy for L, L′ = N becomes nearly the same as that for L, L′ = P at α = 150° and becomes smaller at α = 120°. At α = 90°, one of the NH₃ ligands of (NH₃)₂Pd dissociates. This

result supports the speculation by experimentalists that the nitrogen ligand rather than the phosphine ligand tends to dissociate to prepare a vacant site.[8c] The stronger the electron donation from the LH₃ ligand, the more stabilized the linear structure. However, the stronger the electron donation from the LH₃ ligand, the more destabilized the bent structure, because the electron donation to the dσ+sp hybridized valence orbital of the Pd in the linear structure causes an attractive interaction while the electron donation to the occupied dπ orbital of the Pd in the bent structure causes a repulsive interaction, as illustrated below.
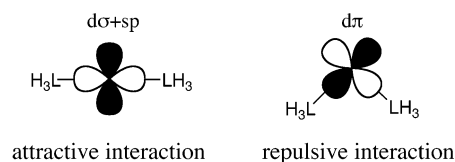
The relative energy shows that the destabilization of (LH₃)(L′H₃)Pd by the bend of the L−Pd−L′ axis is the largest in the case of L, L′ = N, and it is reduced in the order N > P > As > Sb except for the value at α = 90° in the case of L, L′ = Sb. That is, the bend of the L−Pd−L′ axis is easier in the order Sb > As > P > N, because the ability of the electron donation is lower in the reverse order.
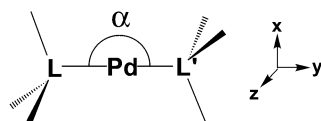
The energy of selected molecular orbitals (MO) of (LH₃)(L′H₃)Pd, which is an important factor to determine the activation mechanism, is also presented in Table 4. These molecular orbitals are lying higher in energy in the order N > P > As > Sb. The bend of the L−Pd−L′ axis stabilizes the valence sp$_x$ hybridized orbital and destabilizes the d$_{xy}$ orbital, as is already well-known.[18] The electronic nature of the (LH₃)(L′H₃)Pd fragments that depends on the atom L affects the activation mechanism as mentioned later.

3.1. Activation of the Sn−C σ-Bond of SnH₃C≡CH. The optimized structures of the intermediates, the transition states, and the products of the activation of the Sn−C σ-bond of SnH₃C≡CH by (LH₃)₂Pd (L = P, As, Sb) complexes are presented together with their potential energy surfaces in Figure 1. In all cases of L = P, As, and Sb, the activation proceeds by two steps passing through the intermediate **2**. The SnH₃C≡CH substrate approaches perpendicularly to the L−Pd−L plane, and the C¹ atom bonded to the Sn coordinates to the Pd in the equatorial plane to form the intermediate **2**. The Sn atom occupies the apical position. The coordinated substrate in **2** starts the rotation around the Pd−C¹ axis. The Sn−C σ-bond is broken during the rotation, and the product **3** that has a square-planar structure is finally formed. The first step of the formation of **2** was followed by optimizing the SnH₃C≡CH-coordinated structure at a variety of L−Pd−L angles α (Table 5). The Sn−C σ-bond approaches Pd in a η^2-fashion with a decrease in the angle α. In the initial stage, the Pd−Sn distance is shorter than the Pd−C¹ distance. The positively charged Sn atom first approaches the negatively charged Pd by an electrostatic interaction. In the case of L = P, the Pd−C¹ distance is

(16) Glendening, E. D.; Reed, A. E.; Carpenter, J. E.; Weinhold F. *NBO Version 3.1.*

(17) The sequence in the electronegativity (in the Pauling's value) of the N, P, As, and Sb atoms is as follows: N (3.04) > P (2.19) ≥ As (2.18) > Sb (2.05). The electronegativity of the H atom is 2.20. For example, see: *The Elements*, 3rd ed.; Emsley, J., Ed.; Oxford University Press: New York, 1998.

(18) (a) Saillard, J.-Y.; Hoffmann, R. *J. Am. Chem. Soc.* **1984**, *106*, 2006. (b) Albright, T. A.; Burdett, J. K.; Whangbo, M. H. In *Orbital Interactions in Chemistry*; Wiley: New York, 1985.

Table 4. Bond Distance and Bonding Energy of Pd−L, Relative Energy (RE), and Molecular Orbital (MO) Energies of the (LH₃)(L′H₃)Pd (L, L′ = N, P, As, Sb) Complexes with a Variety of Angles α at the B3LYP/BSI Level[a]

	Pd−L		RE	MO energy			
α (deg)	distance (Å)	bonding energy[b] (kcal/mol)	(kcal/mol)	d_{z^2}	d_{xz}	d_{xy}	val. sp_x
			L, L′ = N				
180	2.116	31.7	0.0	−0.13443	−0.13441	−0.14977	0.02159
150	2.161, 2.162	24.8	7.4	−0.13221	−0.13229	−0.13612	0.01781
120	2.277, 2.269	11.2	22.5	−0.12012	−0.12545	−0.10915	0.00750
			L = N, L′ = P[c]				
180	2.166/2.316	27.7/32.3	0.0	−0.15701	−0.15699	−0.17828	0.01465
150	2.198/2.328	23.5/28.2	4.5	−0.15754	−0.15743	−0.16671	0.01344
120	2.285/2.359	13.9/19.5	14.6	−0.15387	−0.15853	−0.14315	0.01856
90	2.452/2.400	3.8/11.8	25.4	−0.15461	−0.15685	−0.13281	−0.02168
			L, L′ = P				
180	2.374	26.3	0.0	−0.17346	−0.17346	−0.19550	−0.00217
150	2.376, 2.378	24.4	2.1	−0.17197	−0.17869	−0.19052	−0.00518
120	2.394, 2.400	18.5	8.3	−0.17931	−0.18922	−0.17268	−0.01523
90	2.451, 2.485	11.6	19.1	−0.18123	−0.19469	−0.15978	−0.03047
			L, L′ = As				
180	2.447	23.9	0.0	−0.18202	−0.18202	−0.20780	−0.01391
150	2.448, 2.447	22.6	1.4	−0.18239	−0.18798	−0.20009	−0.01686
120	2.465, 2.459	18.2	4.7	−0.19015	−0.19957	−0.18416	−0.02585
90	2.550, 2.517	9.5	9.8	−0.19196	−0.20500	−0.17179	−0.04006
			L, L′ = Sb				
180	2.588	22.1	0.0	−0.19252	−0.21797	−0.21797	−0.03376
150	2.586, 2.587	21.6	0.5	−0.19532	−0.19942	−0.21113	−0.03429
120	2.596, 2.592	18.9	3.5	−0.20388	−0.21283	−0.19710	−0.03756
90	2.649, 2.687	10.5	13.0	−0.20597	−0.21885	−0.18533	−0.04956

[a] The geometry optimization was performed with D_{2h} symmetry for α = 180° and C_s symmetry for α = 150°, 120°, and 90°. [b] The bonding energy of the Pd−L that has the longer Pd−L distance is presented. [c] The numbers on the left- and right-hand sides of the slash are for Pd−N and Pd−P, respectively.

shortened to 2.567 Å and becomes shorter than the Pd−Sn distance at α = 150°. The electron donation from the highly negatively charged C^1 atom to the valence sp_x hybridized orbital of the Pd is strengthened, because the valence sp_x hybridized orbital is stabilized by the bend of the P−Pd−P axis (see Table 4). On the other hand, the electron back-donation from the d_{xz} orbital of the Pd to the positively charged Sn atom takes place, so that the perpendicular interaction of the Sn−C σ-bond is maintained. The binding energy of SnH₃C=CH increases to 8.6 kcal/mol at α = 140° by these electron donation and back-donation interactions. The atomic orbital population of the Pd d_{xz} is reduced to 1.917 e by electron back-donation, and the electron is accumulated at the C^1 atom through the Sn atom. Therefore, the negative charge of the C^1 increases to −0.63 e, and the total charge of SnH₃C=CH is negative. The atomic orbital population of the C^1 p_x is especially enlarged, because the π orbital p_x of the C^1 participates in the electron donation to the Pd to from the intermediate **2** in the first step, as the author suggested in a previous paper[5] (see the illustration below). When α becomes less than 130°, the substrate no longer stays in the perpendicular (xz) plane. The Sn−C σ-bond preliminary stretched to 2.123 Å rotates around the Pd−C^1 axis and is broken. The d_{xy} orbital is destabilized enough to break the Sn−C bond by electron back-donation to the Sn−C σ* orbital at α less than 130° (see

Table 4).

donation   back-donation
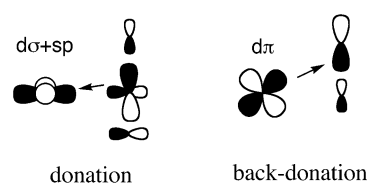
For L = As and Sb, the Pd−C^1 distance is already shorter than the Pd−Sn distance at the large angle α of 160°, and it is shortened to 2.571 Å for L = Sb. This is ascribed to the valence sp_x hybridized orbital for As and Sb that is lying much lower in energy compared with that for P, its energy level being lowered in the order P > As > Sb. The Pd−Sn distance is longer for As and Sb than for P at α less than 160° due to the occupied d_{xz} orbital that is also lying lower in energy for As and Sb than for P. These results are sharply reflected in the binding energy of SnH₃C=CH. For example, the binding energy of SnH₃C=CH is larger for Sb than for P at α = 160°, while it is smaller for Sb than for P at α = 140°. The L−Pd−L′ axis bends enough to attract the Sn−C σ-bond to the Pd in **2**, so that the angle α is reduced to 121.3° for L = Sb. The binding energy of SnH₃C=CH increases to 9−11 kcal/mol for all the cases of L = P, As, Sb. However, the intermediate **2** is the most stable for L = Sb due to the easiness of the bend of the Sb−Pd−Sb axis (see Table 4). Therefore, as shown in Figure 1, when the P atom is replaced by the

Table 5. Change in Geometric Parameters, Relative Energy (RE), Binding Energy (BE), Charges, and Atomic Orbital (AO) Populations with a Decrease in the Angle α on the Perpendicular Approach of $SnH_3C{\equiv}CH$ to the $(LH_3)_2Pd$ Complexes at the B3LYP/BSI Level
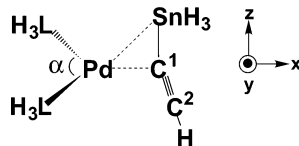
α (deg)	geometric parameters (Å & deg)				RE[a] (kcal/mol)	BE[b] (kcal/mol)	charge			AO population	
	Pd−Sn	Pd−C^1	Sn−C^1	∠Sn−C^1−C^2			Sn	C^1	total[c]	Pd(d$_{xz}$)	C^1(p$_x$)
					L = P						
170	3.624	3.819	2.081	178.1	−1.1	1.8	1.22	−0.54	−0.03	1.957	1.053
160	3.419	3.663	2.082	177.8	−0.5	2.2	1.21	−0.54	−0.04	1.956	1.052
150	3.117	2.567	2.092	169.7	−0.1	4.1	1.22	−0.60	−0.09	1.937	1.053
140	3.040	2.310	2.112	159.4	−0.3	8.6	1.20	−0.63	−0.13	1.917	1.087
130	2.981	2.247	2.123	157.1	−0.1	11.5	1.19	−0.64	−0.14	1.908	1.100
					L = As						
170	3.755	3.922	2.080	178.4	−0.9	1.3	1.22	−0.54	−0.02	1.964	1.050
160	3.419	3.307	2.081	177.8	−0.6	1.7	1.22	−0.55	−0.03	1.962	1.038
150	3.160	2.432	2.097	165.0	−1.2	5.2	1.22	−0.62	−0.09	1.938	1.067
140	3.123	2.332	2.104	162.1	−1.9	7.8	1.22	−0.63	−0.10	1.929	1.081
130	3.109	2.301	2.105	162.6	−2.0	9.3	1.21	−0.63	−0.10	1.925	1.084
					L = Sb						
170	3.997	4.093	2.079	179.0	−0.8	0.9	1.23	−0.55	−0.01	1.975	1.045
160	3.332	2.571	2.090	168.6	−1.1	3.0	1.23	−0.61	−0.05	1.957	1.057
150	3.278	2.401	2.096	164.4	−2.6	5.9	1.23	−0.63	−0.07	1.945	1.076
140	3.273	2.355	2.096	164.8	−3.8	7.5	1.23	−0.63	−0.07	1.940	1.074
121.3[d]	3.013	2.267	2.111	161.7	−4.4	10.7	1.19	−0.64	−0.08	1.948	1.098

[a] Energy relative to the free $(LH_3)_2Pd$ and $SnH_3C{\equiv}CH$. [b] Binding energy of $SnH_3C{\equiv}CH$ with $(LH_3)_2Pd$. See the Computational Procedures for the definition. [c] Total charge of $SnH_3C{\equiv}CH$. [d] Only the $C^1{\equiv}C^2$ π-complex was found at α = 130°.

Sb atom, the exothermicity of the reaction **2** → **TS1** → **3** is reduced to half, and then the transition state **TS1** shifts to the product side, according to the Hammond rule.

Although the activation mechanism for L = N with the high-lying dπ orbital in the N−Pd−N plane is one of our interests, unfortunately the structures at the stationary points could not be optimized. One of the NH_3 ligands dissociates from the Pd atom during the optimization. The reaction was therefore followed by optimizing the structures with a variety of N−Pd−N angles α, assuming a Pd−N distance of 2.116 Å during the reaction.

The incoming substrate $SnH_3C{\equiv}CH$ is attracted to the Pd atom through the interaction of the positively charged Sn atom with the Pd atom in the initial stage of the reaction, as shown in Figure 2. Here, the atomic orbital population of the dσ orbital of the Pd is reduced to 1.649 e by electron transfer to the Sn−C σ* orbital, and the Sn−C bond is stretched to 2.110 Å. At α = 146°, the C^1 atom as well as the Sn atom is strongly attracted to the Pd, and the Sn−C σ-bond is substantially broken in the N−Pd−N plane. The Sn−C σ-bond never undergoes perpendicular coordination throughout the reaction.

On the other hand, for the palladium complex with the hybrid ligand, $(NH_3)(PH_3)Pd$, the structures of the intermediate, the transition state, and the product were successfully obtained by the full optimization. In this case, two possible paths exist, which depend on the position of the Sn atom in the product, i.e., cis or trans to the N, as presented in Figure 3. In both cases, the Sn−C-coordinated intermediate **2** found for $(PH_3)_2Pd$ did not exist. Activation of the Sn−C σ-bond occurs in the N−Pd−P plane by the parallel approach starting

from the $C{\equiv}C$ π-complex **4**. The high-lying d$_{xy}$ orbital of the Pd is a dominant factor that determines the mechanism. The Sn−C σ-bond is strongly attracted parallel to the N−Pd−P plane by electron back-donation from the Pd d$_{xy}$ orbital to the σ* orbital of the Sn−C bond. The negatively charged C^1 atom stays in the proximity of the Pd during the reaction through electron donation to Pd.

We can recognize the trans influence in the transition states **TS1**. In **TS1NP**, where the C^2 atom is trans to the NH_3 ligand, the C^2 atom is still attracted to the Pd atom with a short Pd−C^2 distance of 2.664 Å, although the Pd−Sn is already shortened to 2.712 Å. In this reaction, the dissociation of the C^2 atom and the association of the Sn atom are considered to be competitive. The electron back-donation from the Pd d$_{xy}$ orbital to the π* orbital of the C^2 atom is promoted by the strongly electron-donative NH_3 ligand trans to the C^2 atom. This interaction by electron back-donation strongly binds the $SnH_3C{\equiv}CH$ substrate in the N−Pd−P plane, as shown by the dihedral angle δ of 0.0°. On the other hand, there is no such interaction in the transition state **TS1PN**, where the C^2 atom is trans to the PH_3 ligand. The C^2 atom is located far away from the Pd atom, and the substrate $SnH_3C{\equiv}CH$ is rotated out from the N−Pd−P plane by 45.2°. In both paths, **4NP** → **TS1NP** → **3NP** and **4PN** → **TS1PN** → **3PN**, the activation of the Sn−C σ-bond essentially proceeds in the N−Pd−P plane in one step starting from the $C{\equiv}C$ π-complex **4**. This is similar to the conventional homolytic cleavage of the σ-bond. Thus, the replacement of only one PH_3 ligand by the NH_3 ligand completely changes the activation mechanism.

The energy of both transition states **TS1PN** and **TS1NP** is higher than the reactant **1**, in contrast to the
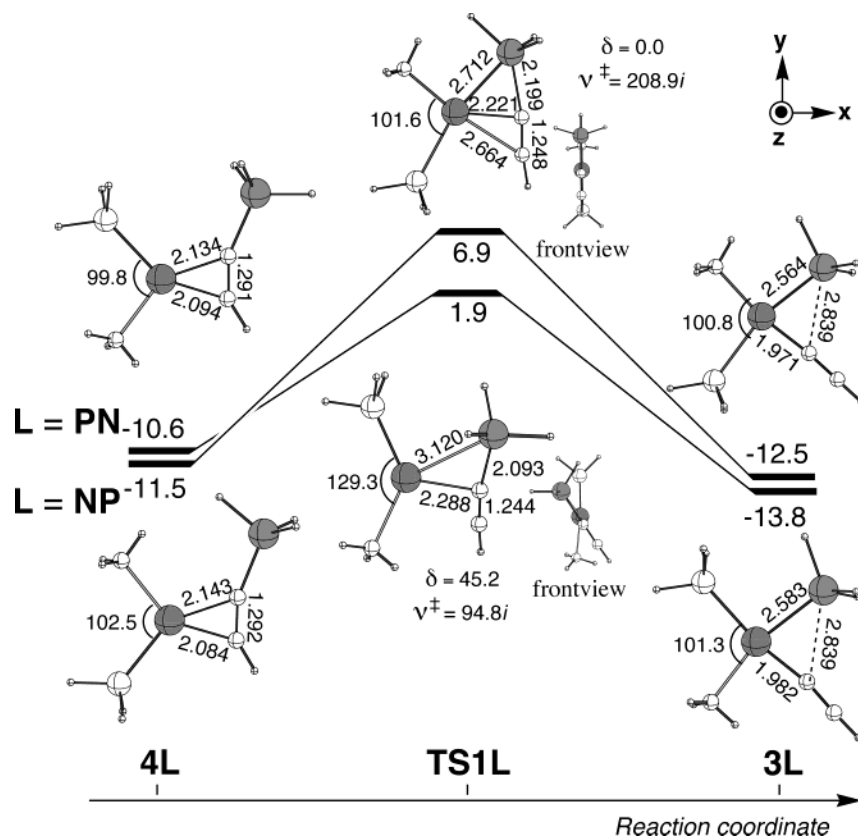
Figure 3. B3LYP/BSII potential energy surfaces (in kcal/mol) of the oxidative addition of the Sn−C σ-bond of SnH$_3$C≡CH to the (LH$_3$)(L′H$_3$)Pd (L = N, L′ = P) complexes **1**, together with the optimized structures (in Å and deg) of the intermediates **4**, the transition states **TS1**, and the products **3** at the B3LYP/BSI level. The imaginary frequency (in cm^{-1}) is shown for the transition states **TS1**. δ represents the dihedral angle $\angle$L(L′)−m−Pd−Sn (m is the midpoint between the L and the L′ atoms).

case of L = P, As, and Sb. The energy barrier is higher by 5.9 kcal/mol for the path **4NP → TS1NP → 3NP** than for the path **4PN → TS1PN → 3PN**. This is ascribed to the following facts: (i) SnH$_3$C≡CH experiences structural stress in the transition state **TS1NP** due to the strong attractive interaction of the C^2 with Pd; (ii) the electron back-donation to the Sn trans to the PH$_3$ ligand is weak.

The activation of the (LH$_2$C$_2$H$_4$LH$_2$)Pd complex with the chelate ligand also occurs in the L−Pd−L plane starting from the C≡C π-complex for both L = N and P, as shown in Figure 4. This is reasonable because the occupied d$_{xy}$ orbital in the L−Pd−L plane is already destabilized enough to interact with the Sn−C σ* orbital by the small L−Pd−L bite angle before the reaction starts. On the other hand, the valence sp$_x$ hybridized orbital is stabilized to interact with the Sn−C σ orbital. In the case of L = N, the dissociation of the C^2 from the Pd and the association of the Sn to the Pd are considered to be competitive on the basis of the structure of the transition state **TS1cN**, as mentioned above. The interaction of the substrate with the Pd in the L−Pd−L plane through the Pd d$_{xy}$ orbital is stronger for L = N than for L = P, as is reflected in the distances between the Pd and the substrate in the π-complexes **4**, the transition states **TS1**, and the products **3**. Consequently, the entire potential energy surface is much lower in energy for L = N than for L = P.

Here, one would be interested in the shape of the potential energy surface of the Sn−C σ-bond activation on the (PH$_2$C$_2$H$_4$PH$_2$)Pd complex by the perpendicular

approach. The dotted line in Figure 4 represents the potential energy surface for the perpendicular approach estimated by replacing two PH$_3$ ligands by the chelate ligand PH$_2$C$_2$H$_4$PH$_2$ in the path **2P → TS1P → 3P**. According to this, the reaction would be downhill when the Sn−C σ-bond activation takes place by the perpendicular approach on the (PH$_2$C$_2$H$_4$PH$_2$)Pd complex.

3.2. Activation of the Sn−C σ-Bond of SnH$_3$(H)-C=CH$_2$. Even if the activation of the Sn−C σ-bond starts from a CC π-complex, the apical site of the palladium complex participates and plays an important role in the activation in some cases.[6,7] In this section, the mechanism of such Sn−C σ-bond activation is discussed in detail using the substrate SnH$_3$(H)C=CH$_2$ as a model.

Not the η^2-Sn−C complex but the C=C π-complex is the starting complex in the activation of the Sn−C σ-bond of SnH$_3$(H)C=CH$_2$ by the (PH$_3$)$_2$Pd complex, as displayed in Figure 5. The C^1 atom tightly binds to the Pd and never dissociates during the reaction. Starting from the π-complex **5**, the Pd−C^2 distance is elongated, and simultaneously the Pd−Sn distance is shortened. Here, the C^1 and the Sn atoms occupy the equatorial and the apical positions, respectively, by electron donation from the highly negatively charged C^1 atom to the valence sp$_x$ hybridized orbital of the Pd and the electron back-donation from the Pd d$_{xz}$ orbital to the positively charged Sn atom, as mentioned above. This is a peculiar behavior of the highly polarized Sn−C σ-bond. In the case of CH$_3$(H)C=CH$_2$, the C=C double bond first dissociates completely from the Pd, and then the non-

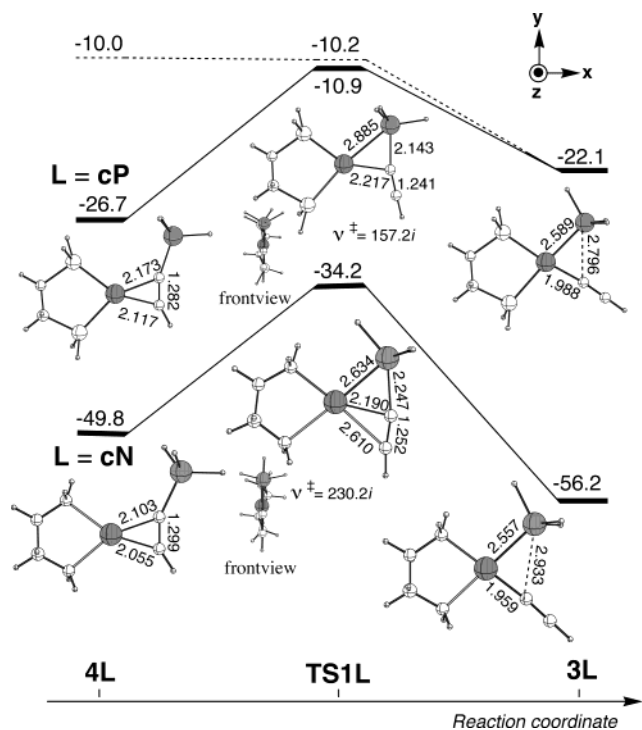**Figure 4.** B3LYP/BSII potential energy surfaces (in kcal/mol) of the oxidative addition of the Sn−C σ-bond of SnH$_3$C≡CH to the (LH$_2$C$_2$H$_4$LH$_2$)Pd (L = N, P) complexes **1**, together with the optimized structures (in Å and deg) of the intermediates **4**, the transition states **TS1**, and the products **3** at the B3LYP/BSI level. The potential energy surface drawn by the dotted line was calculated by replacing two phosphine ligands of the intermediate **2P** and the transition state **TS1P** of the path **2P → TS1P → 3P** by the chelate ligand PH$_2$C$_2$H$_4$PH$_2$. The imaginary frequency (in cm^{-1}) is shown for the transition states **TS1**.

polar C−C σ-bond approaches the Pd parallel to the P−Pd−P plane. The C−C σ-bond is on the P−Pd−P plane throughout the activation reaction.

The Sn−C σ-bond perpendicularly coordinated to the (PH$_3$)$_2$Pd in a η^2-fashion rotates around the Pd−C^1 axis, which is similar to the case of SnH$_3$C≡CH. One would notice here that there are two kinds of rotation of the substrate, as presented below.
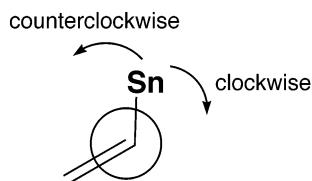
One is clockwise rotation, and the other is counterclockwise rotation. Therefore, two paths, a and b, which have the same reactant and the product, exist, as presented in Figure 5. We can find the crucial difference in the position of the C^2 atom during the rotation between paths a and b. In path a, with clockwise rotation, the C^2 atom immediately moves away from the Pd just after the rotation starts. In contrast to this, the C^2 atom stays in the vicinity of the Pd with a distance of about 2.9 Å until the end of the Sn−C σ-bond breaking in path b, with counterclockwise rotation. The lobe of the π* orbital of the C^2 atom is always directed toward the Pd atom to interact in path b. The C^2 atom as well as the Sn

atom interacts with the Pd through electron back-donation from the Pd d$_{xz}$ or d$_{z^2}$ orbital. This attractive interaction would lower the transition state in path b, as shown in Figure 5. As a result, path b, with counterclockwise rotation, is energetically more favorable than path a, with clockwise rotation.

In fact, not only the Sn−C σ-bond but also the C≡C π-bond of SnH$_3$C≡CH has an attractive interaction with the Pd, even if its molecular axis is perpendicular to the P−Pd−P plane. Their structures are presented in Figure 6 (**TS4P** and **TS5P**). **TS4P** corresponds to the transition state of the path **3P → TS4P → 3P**, where the positions of SnH$_3$ and C≡CH in **3P** are mutually switched. The structural features of **TS4P** are the same as those of the intermediate **2P**, although the Pd−Sn and the Pd−C^1 distances are much shorter due to the strong binding of SnH$_3$C≡CH to the Pd (16.3 kcal/mol, see Table 6). **TS5P** is also the transition state of the path **4P → TS5P → 4P**. The Pd−C distances are stretched by 0.2−0.4 Å in **TS5P** compared with those in **4P**, but those distances are still less than 2.6 Å. The binding energy of SnH$_3$C≡CH in **TS5P** was calculated to be 7.2 kcal/mol (Table 6). Table 6 shows that the electron is donated back from the d$_{xz}$ and the d$_{z^2}$ orbitals of the Pd to the σ* orbital of the Sn−C bond in **TS4P** and to the π* orbital of the C≡C bond in **TS5P**.

Thus, the apical site plays an important role to lower the transition state and determine the reaction path. The same path preference was shown for L = As and Sb (Figure 5). The energy barrier is smaller by about 3 kcal for path b with counterclockwise rotation than for path a with clockwise rotation.

Now, it is a subject of interest whether the nitrogen ligand also indicates the same preference on the activation path, because the apical site of the palladium complex does not participate in the Sn−C σ-bond activation of SnH$_3$C≡CH only for the case of the nitrogen ligand as mentioned in the previous section. The effect of the ligand on the path preference in the Sn−C σ-bond activation of SnH$_3$(H)C≡CH$_2$ was examined using the (LH$_2$C$_2$H$_4$LH$_2$)Pd complex (L = N, P).

Two paths a and b, which are accompanied by the clockwise and the counterclockwise rotation of SnH$_3$-(H)C≡CH$_2$, respectively, were also found for the (PH$_2$C$_2$H$_4$PH$_2$)Pd complex with the chelate ligand, as displayed in Figure 7. Although the entire potential energy surfaces are stabilized by 12−14 kcal/mol, the features of the optimized structures and the shape of the potential energy surfaces are nearly the same as those for (PH$_3$)$_2$Pd. The transition state **TS3cP** of path b is more stable by 5.1 kcal/mol than the transition state **TS2cP** of path a. Therefore, path b, which passes through the lower transition state, is energetically favorable.

On the other hand, the (NH$_2$C$_2$H$_4$NH$_2$)Pd complex unexpectedly has only path b, with counterclockwise rotation (Figure 8). One would predict that the Sn−C σ-bond immediately moves to the N−Pd−N plane without the interaction at the apical site on the basis of the results for the Sn−C σ-bond activation of SnH$_3$C≡CH in the case of the nitrogen ligand presented in the previous section. However, starting from the π-complex **5cN**, the Sn−C σ-bond takes not the shortest way by clockwise rotation but the long way by counterclockwise

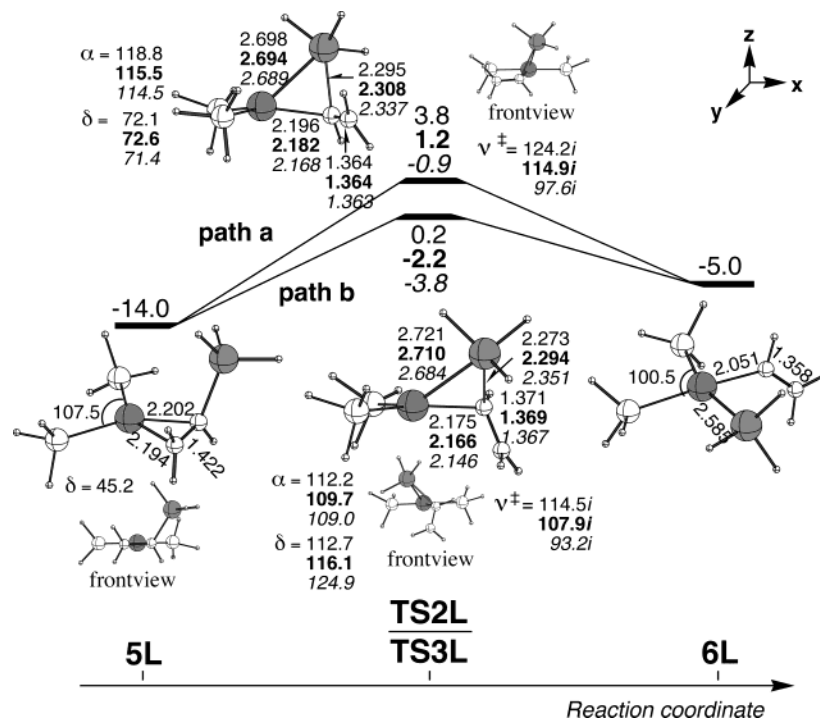**Figure 5.** B3LYP/BSII potential energy surfaces (in kcal/mol) of paths a ($5 \rightarrow$ **TS2** $\rightarrow$ **6**) and b ($5 \rightarrow$ **TS3** $\rightarrow$ **6**) for the oxidative addition of the Sn−C σ-bond of $SnH_3(H)C=CH_2$ to the $(LH_3)_2Pd$ (L = P, As, Sb) complexes **1**, together with the optimized structures (in Å and deg) of the intermediates **5**, the transition states **TS2** and **TS3**, and the products **6** at the B3LYP/BSI level. For L = As and Sb, the structures and the energies only for the transition states **TS2** and **TS3** are presented. In paths a and b, the coordinated substrate $SnH_3(H)C=CH_2$ in **5** rotates clockwise and counterclockwise, respectively. The imaginary frequency (in cm^{-1}) is shown for the transition states **TS2** and **TS3**. α and δ represent the angle $\angle$L−Pd−L and the dihedral angle $\angle$L−m−Pd−Sn (m is the midpoint between two L atoms), respectively. The numbers in normal, bold face, and italic type are for L = P, As, and Sb, respectively.
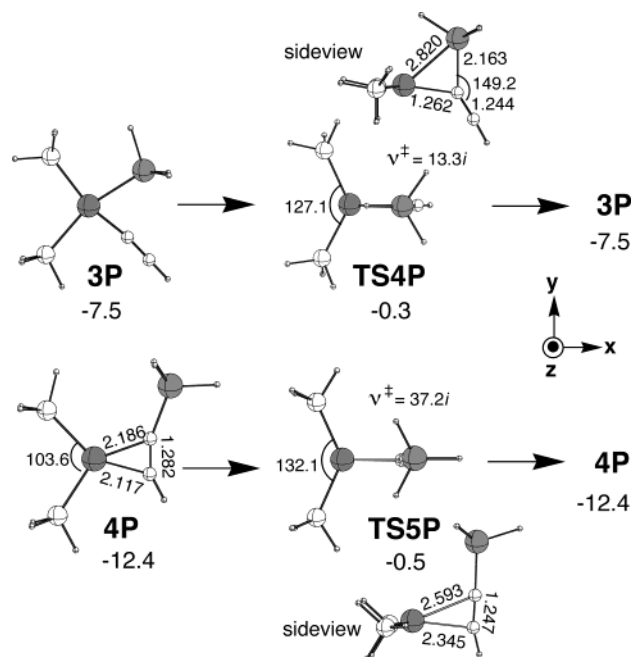

Figure 6. B3LYP/BSI-optimized structures (in Å and deg) and B3LYP/BSII energies (in kcal/mol) for paths of the rotation of $SnH_3C≡CH$ on **3P** and **4P** through the transition states **TS4P** and **TS5P**. All structures have C_s symmetry. The imaginary frequency (in cm^{-1}) is shown for the transition states **TS4P** and **TS5P**.

rotation to make its axis parallel to the N−Pd−N plane (path b). In the transition state **TS3cN**, the Sn−C^1=C^2 skeleton of $SnH_3(H)C≡CH_2$ is completely out of the

Table 6. Change in Atomic Orbital (AO) Populations in the Rotation of $SnH_3C≡CH$ on 3P and 4P, 3P $\rightarrow$ TS4P $\rightarrow$ 3P and 4P $\rightarrow$ TS5P $\rightarrow$ 4P, and Binding Energy (BE) of $SnH_3C≡CH$ on TS4P and TS5P at the B3LYP/BSI Level

	AO population			BE (kcal/mol)
	d_{xz}	d_{z^2}	d_{xy}	
3P	1.97	1.96	1.64	
TS4P	1.93	1.93	1.91	16.3
3P	1.97	1.96	1.64	
4P	1.96	1.95	1.69	
TS5P	1.90	1.93	1.95	7.2
4P	1.96	1.95	1.69	

N−Pd−N plane, and the Sn atom occupies the apical position with the Pd−Sn bond distance of 2.772 Å. Here, it should be noted that the Pd−C^2 bond has a quite short distance of 2.629 Å, which is shorter by 0.206 Å than that for the case of the $(PH_2C_2H_4PH_2)Pd$ complex. As mentioned above, the C^2 atom of $SnH_3(H)C≡CH_2$ stays in the vicinity of the Pd during the activation reaction through electron back-donation from the Pd d_{xz} or d_{z^2} orbital to the π^* orbital of the C^2 atom in path b. We should remember that the nitrogen complex tends to reduce the repulsive interaction between the occupied d orbitals of the Pd and the strongly electron-donative nitrogen ligand by electron back-donation from the occupied d orbitals of the Pd to the antibonding orbitals of the Sn and the C^2 atoms, e.g., see the transition states, **TS1NP** (Figure 3) and **TS1cN** (Figure 4). Also, the d_{z^2} orbital as well as the d_{xz} orbital of the Pd is highly enhanced in energy to interact with those antibonding
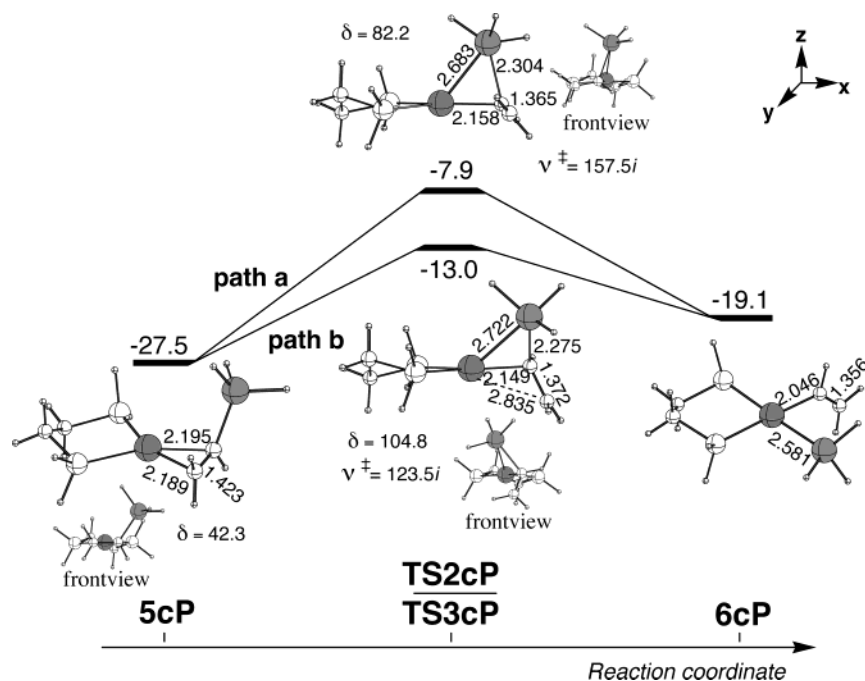
Figure 7. B3LYP/BSII potential energy surfaces (in kcal/mol) of paths a (**5cP** → **TS2cP** → **6cP**) and b (**5cP** → **TS3cP** → **6cP**) for the oxidative addition of the Sn–C σ-bond of $SnH_3(H)C=CH_2$ to the $(PH_2C_2H_4PH_2)Pd$ complex **1cP**, together with the optimized structures (in Å and deg) of the intermediates **5cP**, the transition states **TS2cP** and **TS3cP**, and the products **6cP** at the B3LYP/BSI level. In paths a and b, the coordinated substrate $SnH_3(H)C=CH_2$ in **5cP** rotates clockwise and counterclockwise, respectively. The imaginary frequency (in cm^{-1}) is shown for the transition states **TS2cP** and **TS3cP**. δ represents the dihedral angle ∠P–m–Pd–Sn (m is the midpoint between two P atoms).
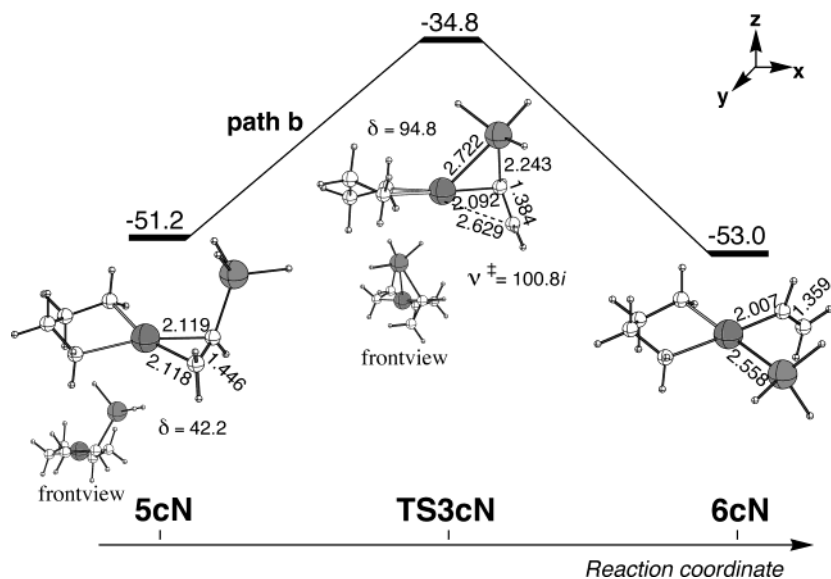

Figure 8. B3LYP/BSII potential energy surface (in kcal/mol) of path b (**5cN** → **TS3cN** → **6cN**) for the oxidative addition of the Sn–C σ-bond of $SnH_3(H)C=CH_2$ to the $(NH_2C_2H_4NH_2)Pd$ complex **1cN**, together with the optimized structures (in Å and deg) of the intermediate **5cN**, the transition state **TS3cN**, and the product **6cN** at the B3LYP/BSI level. In path b, the coordinated substrate $SnH_3(H)C=CH_2$ in **5cN** rotates counterclockwise. The imaginary frequency (in cm^{-1}) is shown for the transition state **TS3cN**. δ represents the dihedral angle ∠N–m–Pd–Sn (m is the midpoint between two N atoms).

orbitals in the case of the nitrogen ligand (see Table 4). This electronic repulsion cannot be reduced enough in path a, because the C^2 atom immediately moves away from the Pd after the activation reaction starts. In contrast, the C^2 atom stays close to the Pd atom until the Sn–C bond is broken in the N–Pd–N plane in path b.

4. Concluding Remarks

The author has reported the importance of the apical site of the palladium complexes on the activation and

the formation of the σ-bond, the insertion reaction, and so on.[5–7,19] The activation of the Sn–C σ-bond of $SnH_3C≡CH$ on the $(PH_3)_2Pd$ complex is one of the typical reactions that proceeds with the support of the apical site.[5] To understand in more detail the essential factor that controls this unique mechanism, the electronic effect on the mechanism of the activation of the highly polarized Sn–C σ-bond was theoretically exam-

(19) (a) Matsubara, T.; Hirao, K. *J. Am. Chem. Soc.* **2002**, *124*, 679. (b) Matsubara, T.; Hirao, K. *Organometallics* **2002**, *21*, 1697.

ined by the density functional method (B3LYP) using model complexes with various ligands, $(LH_3)(L'H_3)Pd$ and $(LH_2C_2H_4LH_2)Pd$ (L, L' = N, P, As, Sb), and the substrates $SnH_3C{\equiv}CH$ and $SnH_3(H)C{=}CH_2$.

The highly polarized Sn−C σ-bond of $SnH_3C{\equiv}CH$ approaches the Pd perpendicularly to the P−Pd−P plane of $(PH_3)_2Pd$, and the activation of the Sn−C σ-bond takes place in two steps via the intermediate **2P**. This is completely different from the conventional activation for the σ-bond such as H−H, C−H, and C−C. In the intermediate **2P**, the polarization of the Sn−C σ-bond is further encouraged by the electron donation from the C atom to the Pd. This is a driving force of the reaction. The highly positively charged Sn atom migrates to the equatorial plane by the rotation of the substrate around the Pd−C axis. This heterolytic activation, which consists of two steps, does not change in the case of $(AsH_3)_2Pd$ and $(SbH_3)_2Pd$. However, when the PH_3 ligand is replaced by the more σ-donative NH_3 ligand, the activation homolytically occurs in the N−Pd−P plane in one step from the π-complex. The $(LH_2C_2H_4LH_2)Pd$ complex with the chelate ligand also showed the same homolytic activation mechanism in both cases of L = N and P.

In the case of the substrate $SnH_3(H)C{=}CH_2$, the activation of the Sn−C σ-bond proceeds with the support of the apical site, although it starts from the C=C π-complex. This activation reaction also leads to a structure with the Sn−C coordinated perpendicularly to the L−Pd−L plane in a η^2-fashion and is accompanied by the rotation of the coordinated $SnH_3(H)C{=}CH_2$. Here, there exist the alternative paths, i.e., path a with clockwise rotation of the coordinated $SnH_3(H)C{=}CH_2$ and path b with counterclockwise rotation of the coordinated $SnH_3(H)C{=}CH_2$. Path b, where the apical site effectively contributes to the reaction, was energetically more favorable for all the ligands, L = N, P, As, and Sb.

Supporting Information Available: Listings giving the optimized Cartesian coordinates of all equilibrium structures and transition states presented in this paper. This material is available free of charge via the Internet at http://pubs.acs.org.

OM0303449